

## 607 6 Supplementary Material

### 608 6.1 Experimental Details

**Table 2:** Model configurations of the large and small models for each evaluation task. For comparison, the number of layers, hidden dimension, FFN dimension, and the number of decoder parameters (without embeddings) for each model are provided.

| Task                | Model          | # Layers | dim  | FFN dim | # Params |
|---------------------|----------------|----------|------|---------|----------|
| Machine Translation | mT5-large [75] | 24       | 1024 | 2816    | 409M     |
|                     | mT5-small [75] | 8        | 512  | 1024    | 25M      |
| Summarization       | T5-large [44]  | 24       | 1024 | 4096    | 402M     |
|                     | T5-small [44]  | 6        | 512  | 2048    | 25M      |

#### 609 6.1.1 Training Details

610 For machine translation, we use IWSLT 2017 German-English [3] and WMT 2014 German-  
611 English [1] as target benchmarks, and mT5 [75] as a target model. We use the 8-layer mT5-small  
612 and the 24-layer mT5-large as the small and large models. For summarization, we use XSUM [40]  
613 and CNN/DailyMail [20] as target benchmarks, and T5 [44] as a target model. We use T5-small  
614 and T5-large with 6 and 24 layers, respectively, for the small and large models. Table 2 summarizes  
615 the size and configuration of each model. All the models are fine-tuned from the pre-trained check-  
616 points of the HuggingFace library [70] for 500k steps using a batch size of 16. We use Adafactor  
617 optimizer [50] with constant learning rate of  $\{0.5, 1, 2, 5\}e-4$  for the small models and  $\{0.5, 1\}e-4$   
618 for the large models. We refer to the normally fine-tuned models on the validation datasets as the  
619 *baseline* small and large models.

620 When training *aligned* small models via the prediction alignment method described in Section 3.5.1,  
621 we first generate calibration datasets using the input sequences from the training datasets of each  
622 benchmark. We then use the fully trained large model to generate output sequences through greedy  
623 sampling with a beam size of 1. To ensure a fair comparison, we fine-tune pre-trained small models  
624 (rather than the baseline small models that are already fine-tuned on the training datasets) on the  
625 calibration datasets using the same training recipes and the number of training steps as described  
626 above. This decision is based on our observation that fine-tuning a baseline model using the calibration  
627 dataset tends to improve generation quality, likely due to the increased number of training examples  
628 and data augmentation effects, which makes it difficult to make a fair comparison between unaligned  
629 BiLD and aligned BiLD. However, in practice, one can obtain aligned models by applying the  
630 prediction alignment method directly to the fine-tuned baseline small models to achieve the best  
631 performance.

#### 632 6.1.2 Evaluation Details

633 All inference evaluations including latency measurement are conducted on a single NVIDIA T4 GPU  
634 of a GCP n1-standard-4 instance with 4 vCPUs and 15GB memory. For inference, we use batch  
635 size 1, which is a common use case for online serving [48]. For the distance metric  $d$  in Equation 3  
636 for the rollback policy, we use the cross-entropy loss between the small model’s hard label and the  
637 large model’s soft label. This measures the (negative log) likelihood of obtaining the small model’s  
638 prediction from the large model’s output. For BiLD inference, we sweep over different fallback  
639 and rollback thresholds to explore different trade-offs between generation quality and latency. For  
640 the machine translation tasks, we use fallback thresholds in  $[0.5, 0.9]$  and rollback thresholds in  $[1,$   
641  $10]$ . For the summarization tasks, fallback thresholds in  $[0.2, 0.6]$  and rollback thresholds in  $[2, 6]$ .  
642 We keep the maximum generation length of the small model to 10 to avoid high rollback costs. In  
643 Appendix 6.3.3, we provide a detailed analysis of how varying the fallback and rollback thresholds  
644 impacts the trade-offs between generation quality and latency in the BiLD framework.

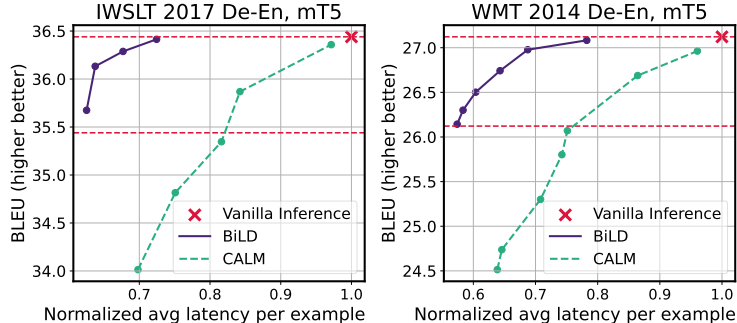


**Figure 7:** The trade-off curves between inference latency and BLEU score for BiLD and CALM in the early exiting setting for (Left) IWSLT 2017 De-En and (Right) WMT 2014 De-En. The  $\times$  marks indicate the vanilla inference latency and BLEU score of the mT5-small models. The horizontal lines indicate the vanilla inference score and 1 point degradation from it. BiLD outperforms CALM across all speedup regimes by up to 2  $\sim$  2.5 points better BLEU score, demonstrating the effectiveness of our approach for the early exiting strategy.

645 **6.2 Details of Early Exiting Strategy in the BiLD Framework**

646 **6.2.1 Training and Evaluation Details**

647 **BiLD.** We use the mT5-small model as the large model and the first (out of 8) layer as the small  
 648 model, and evaluate it on two machine translation benchmarks: IWSLT 2017 De-En and WMT 2014  
 649 De-En. To ensure consistency between the prediction made after the first layer and the one made  
 650 after the last layer, we fine-tune the pre-trained mT5 model using the average loss of the first and  
 651 the final layers, similar to [10, 48]. That is,  $\mathcal{L} = \frac{1}{2}(\mathcal{L}_1 + \mathcal{L}_{-1})$  where  $\mathcal{L}_1$  and  $\mathcal{L}_{-1}$  are the negative  
 652 log-likelihood loss after the first layer and the final layer. The prediction head is shared for these two  
 653 layers. We fine the pre-trained mT5-small model on each benchmark for 500k steps using a batch size  
 654 of 16. Similar to the main experiments, we use Adafactor optimizer [50] with constant learning rate  
 655 of  $\{0.5, 1, 2, 5\}e-4$ . For evaluation, we use fallback thresholds in  $[0.2, 0.8]$  and rollback thresholds  
 656 in  $[0.5, 1.5]$ .

657 **CALM.** To reproduce CALM [48] in our experimental setup, we have fine-tuned the pre-trained  
 658 mT5-small model on IWSLT 2017 De-En and WMT 2014 De-En datasets. We employ the averaged  
 659 loss across all layers, i.e.,  $\mathcal{L} = \sum_{i=1}^L w_i \mathcal{L}_i$ , where  $w_i = i / \sum_{j=1}^L j$ , which was introduced in the  
 660 paper to ensure the layer consistency. We use Adafactor optimizer [50] with constant learning rate  
 661 of  $\{0.5, 1, 2, 5\}e-4$  for 500k training steps. To make a fair comparison, we match the BLEU  
 662 score of the fine-tuned model to that of BiLD’s models Among the two training-free confidence  
 663 measures introduced in the CALM paper, softmax-based and hidden-state saturation-based measures,  
 664 we have chosen to use the latter approach as an early exiting criterion. That said, if the cosine  
 665 similarity between the current layer’s hidden states and the previous layer’s hidden states exceeds a  
 666 certain threshold, we perform early exiting. We have found that the softmax-based alternative is not  
 667 applicable in our evaluation scenario due to the large output vocabulary (more than 200k for mT5,  
 668 which is  $\sim 10\times$  larger than T5), which significantly increases latency overhead. As described in  
 669 the paper, when early exiting happens, the hidden states of the exited layer are propagated down to  
 670 the remaining layers to compute the key and value caches. To achieve different trade-offs between  
 671 latency and generation quality, we sweep over  $\lambda$  in  $[0.7, 0.98]$  and  $t$  in  $\{0, 1, 2, 4, 8\}$  in the decaying  
 672 threshold function.

673 **6.2.2 Performance Comparison between BiLD and CALM**

674 Figure 7 illustrates the BLEU score and latency curves of BiLD compared to CALM in the early  
 675 exiting setting. In both tasks, our method achieves significantly better BLEU scores with the same  
 676 latency speedup, yielding up to around 2 point better BLEU score in the  $\sim 1.5\times$  speedup regime.  
 677 This can be attributed to two factors. First, in BiLD, even if an early exited prediction (i.e., prediction  
 678 made by the smaller model) is incorrect, it can be corrected and replaced using the rollback policy.  
 679 Therefore, an error in the early exited layer is propagated less drastically to the future prediction.

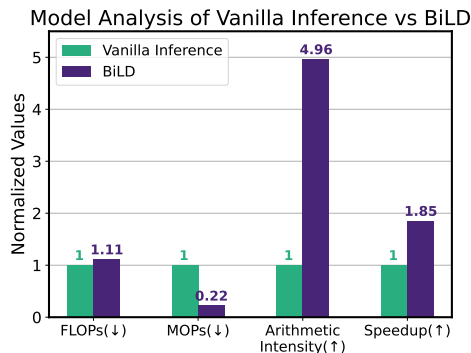


**Figure 8:** FLOPs, MOPs (memory operations), arithmetic intensity, and latency speedup comparison of vanilla inference and BiLD. BiLD approach results in a remarkable reduction in MOPs due to the improved token-level parallelism, resulting in significantly higher arithmetic intensity.

680 Second, the key and value caches for skipped layers are filled with actual values instead of being  
 681 computed from the exiting layer’s hidden states. This also leads to reduced error propagation and  
 682 improved decoding stability.

### 683 6.3 Additional Analysis

#### 684 6.3.1 Model Analysis of BiLD: FLOPs, MOPs, and Arithmetic Intensity

685 Figure 8 compares average FLOPs, MOPs (memory operations), arithmetic intensity, and the latency  
 686 speedup of the vanilla inference and BiLD on the CNN/DailyMail benchmarks. For BiLD, we use  
 687 the model with roughly the same ROUGE-L score as the vanilla inference, and all the numbers  
 688 are normalized by the numbers of the vanilla inference. The figure illustrates that BiLD exhibits  
 689 slightly higher FLOPs compared to the vanilla inference. This is due to the fact that the autoregressive  
 690 and non-autoregressive executions have the same amount of FLOPs, and BiLD involves additional  
 691 overhead of running the small model alongside. However, in the case of MOPs, BiLD demonstrates a  
 692 significant  $\sim 5\times$  reduction of memory operations. This can be attributed to the capability of BiLD  
 693 to process multiple tokens with a single weight load, thereby enhancing token-level parallelism  
 694 and maximizing data reuse. In contrast, this is not the case in the vanilla inference where a single  
 695 weight load can only process a single token. Consequently, BiLD achieves a significantly higher  
 696 arithmetic intensity, which is approximately 5 times larger than the vanilla inference. Arithmetic  
 697 intensity [69] measures the number of arithmetic operations that can be performed per memory  
 698 operation. Given that memory operations can contribute more to the overall inference latency than  
 699 arithmetic operations in many Transformer decoding scenarios [30], decreasing memory operations  
 700 and increasing arithmetic intensity can effectively alleviate the inference bottleneck. This leads to an  
 701 overall latency speedup of  $1.85\times$  on actual hardware.

#### 702 6.3.2 Examples of Generated Sequences

703 Figure 9 provides examples of text sequences generated by BiLD on the validation set of IWSLT  
 704 2017 De-En, along with the ground truths (i.e., labels) and outputs of the pure large and small  
 705 baseline models. The tokens generated from the large model of BiLD are highlighted in green, while  
 706 all the other tokens are generated by the small model. The results illustrate that the small model  
 707 often produces low-quality texts, by predicting inaccurate tokens which can alter the meaning of  
 708 the entire sentence. To contrast, it is observed from the examples that BiLD is able to improve the  
 709 text generation quality by letting the large model interrupt when the small model generates incorrect  
 710 tokens. Particularly, in the examples provided, BiLD tends to be as strong as the large model at  
 711 predicting terminologies. Overall, the large model’s engagement in BiLD decoding not only improves  
 712 the prediction accuracy but also prevents incorrect predictions from impacting the future ones.

|                     |  |
|---------------------|--|
| <b>Ground Truth</b> | And Siftables are an example of a new ecosystem of tools for manipulating digital information.                         |
| <b>Large</b>        | And the Siftables are an example of a new generation of manipulation tools for digital data.                           |
| <b>Small</b>        | And the if you look at the ifeses are an example of a new generation of technologies for manipulation of digital data. |
| <b>BiLD (ours)</b>  | And the <b>Siftables</b> are an example of a new generation of <b>manipulation of</b> digital data.                    |
| <br>                |  |
| <b>Ground Truth</b> | Which is great, because the Romans did not actually think that a genius was a particularly clever individual.          |
| <b>Large</b>        | That's great. The Romans didn't really think that a genius was a particularly smart individual.                        |
| <b>Small</b>        | That's great. The tube didn't really think that a genius was a particularly lonely individual.                         |
| <b>BiLD (ours)</b>  | That's great. The <b>Romans</b> didn't really think that <b>a</b> genius was a particularly smart individual.          |
| <br>                |  |
| <b>Ground Truth</b> | The viral particles then were released from the cells and came back and killed the E. coli.                            |
| <b>Large</b>        | The viral particles then were released by the cells and came back and killed E. coli.                                  |
| <b>Small</b>        | The viral particles were then released by the cells and came back and killed E. Coke.                                  |
| <b>BiLD (ours)</b>  | The viral particles <b>then were</b> released <b>by the</b> cells and came back and killed E. <b>coli</b> .            |

**Figure 9:** Example text sequences that BiLD generates with the validation set of IWSLT 2017 De-En, compared to the ground truths and the outputs of the large and small baselines. For BiLD, tokens generated by the large model are highlighted in red, while all the other tokens are generated by the small model. This illustrates that with a small engagement of the large model, BiLD can correct not only inaccurate vocabulary but also wrong semantics of the text that the small model would have otherwise generated.

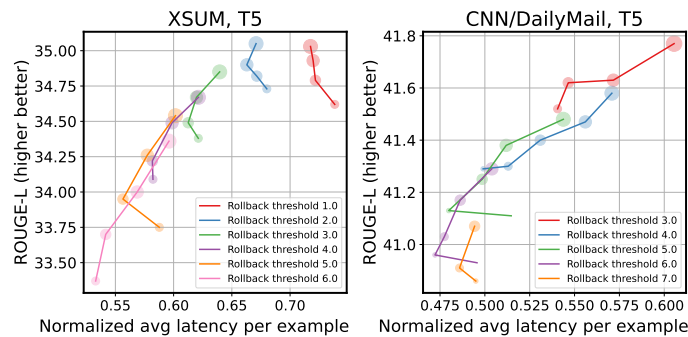


**Figure 10:** The trade-off between latency and generation quality (ROUGE-L) for the aligned BiLD model on two summarization tasks: (Left) XSUM and (Right) CNN/DailyMail. Each curve represents a different rollback threshold, with smaller thresholds indicating more rollbacks. The trade-off can be further obtained within each curve with different fallback thresholds, where larger scatter sizes indicate larger fallback thresholds. A larger fallback threshold implies more fallbacks.

### 713 6.3.3 Impact of Fallback and Rollback on Performance

714 We have explored how the BiLD framework can achieve different trade-offs between latency and  
715 generation quality by adjusting fallback and rollback thresholds. In this section, we present a detailed  
716 analysis of how these thresholds affect the performance using the aligned BiLD model on two  
717 different summarization tasks, XSUM and CNN/DailyMail, as illustrated in Figure 10. Different  
718 curves in the plot represent different rollback thresholds, and each scatter point within the curve  
719 represents different fallback thresholds. Note that a small rollback threshold implies more rollback,  
720 while a larger fallback threshold implies more fallback.

721 We observe a general trend where smaller rollback thresholds (i.e., more rollbacks) result in better  
722 generation quality but longer latency. This trend is expected because, with more rollback, we preempt  
723 more small model's predictions that can be potentially inaccurate by sacrificing the latency. Similarly,  
724 there is also a general trend that smaller fallback thresholds (i.e., fewer fallbacks) result in faster  
725 latency but a worse generation quality. However, we observed that lowering the fallback rates beyond  
726 a certain point can actually hurt both the latency and generation quality. This is because inaccurate  
727 predictions that the small model should have fallen back are later rolled back, incurring an extra  
728 'flush' cost for the tokens that follow.